JOURNAL OF CATALYSIS **175,** 27–39 (1998)
ARTICLE NO. CA981976

Mo–V–Nb Oxide Catalysts for the Partial Oxidation of Ethane

II. Chemical and Catalytic Properties and Structure Function Relationships

K. Ruth,* R. Burch,* and R. Kieffer†

*Catalysis Research Centre, Department of Chemistry, The University of Reading, Whiteknights, Reading RG6 6AD, England; and †L.E.R.S.I., École Européenne de Chimie Polymères Matériaux de Strasbourg, 1, Rue Blaise Pascal-B. P. 296, 67008 Strasbourg cedex, France
E-mail: scsburch@reading.ac.uk

Received July 21, 1997; revised October 28, 1997; accepted November 27, 1997

A mixed oxide catalyst of the composition Mo(73)V(18)-Nb(9)O(x) and crystalline phases prepared in pure form were analysed for their acidity and reducibility. The results were used to find possible relationships between these properties and the catalytic activity of the samples, determined under a reaction pressure of 2 MPa, for the selective oxidation of ethane to ethene and acetic acid and for the formation of acetic acid from ethene. Effects of the morphology and elemental distribution of these samples, as described elsewhere, have also been considered. While all samples catalysed the oxidative dehydrogenation of ethane to ethene, only the $Mo_6V_9O_{40}$ phase and the multiphase catalyst, the two most easily reduced samples, led to the formation of acetic acid. This suggests that the oxygenation to acetic acid is favoured over an easily reducible catalyst. The selectivities and ethane conversion obtained with the multiphase catalyst were found to be higher than with any of its crystalline components. Therefore, the amorphous part of the multiphase catalyst seems to be particularly important. For the oxidation of ethene, the acetic acid yield was highest when catalysed by the $Mo_6V_9O_{40}$ phase. It is proposed that this result is related to the higher acidity relative to the multiphase catalyst, thereby supporting the view that the activation of the hydrocarbon occurs by heterolytic splitting of the C–H bond.

1. INTRODUCTION

Mo–V–Nb oxide catalysts are known to be active for the oxidative dehydrogenation and partial oxidation of ethane (1–4). In the previous publication (5) the preparation and structural characterisation of a multiphase catalyst and a number of specially selected crystalline phases were described. This multiphase catalyst is known to catalyse the oxidative dehydrogenation of ethane to ethene as well as the oxidation to acetic acid. In the present paper the chemical characterisation and the catalytic properties of the materials under a range of reaction conditions is presented and this information, together with the structural characterisation information, is used to explore possible relationships between the catalytic properties and the structural and chemical characteristics of the materials for the selective oxidation of ethane to ethene and oxygenates.

2. EXPERIMENTAL

For the temperature-programmed reduction (TPR) measurements the samples were first heated up to 150°C under helium to desorb water from the surface. The reducibility measurements were then accomplished by heating the sample (sample mass: 50 or 200 mg) at a heating rate of 15°C/min under a diluted or pure hydrogen stream (6.5%, 30%, 100%; balance: helium) and detecting the water formed with a thermal conductivity detector (TCD). The signal from the TCD was taken as a measure for the oxygen removed from the catalyst.

The temperature-programmed desorption of NH_3 was used to determine the acidity of the samples. Although this method does not give exact values for acid strength, it allows a ready comparison of the acidity of different samples. The number of acid sites is related to the amount of desorbed NH_3, whereas the desorption temperature gives information about the acid strength (6). For these measurements the samples were first held at 350°C for one hour in a helium stream to desorb gas molecules from the sample surface. After that a diluted ammonia stream (5% NH_3, 95% He) was passed over the sample at 50°C for 30 min. The reactor was then cooled down to room temperature and purged with helium for 40 min to remove residual, unadsorbed ammonia before heating at 10°C/min under helium. Desorbed NH_3 was detected using a mass spectrometer.

For catalytic measurements with ethane 1.8-g samples were taken. A tubular reactor (inner diameter: 4 mm), made of stainless steel with a glass lining, was used. The compositions and flow rates of the input gases (air and ethane, purity: commercial grade) were controlled by mass flow controllers. The flow rate was 24 cm^3/min while the volume ratio air : ethane was 3 : 1. The pressure was varied in the range of atmospheric pressure to 2 MPa, the

0021-9517/98 $25.00

minimum reaction temperature was 180°C. The dwell time at each temperature was 12 h, taking measurements every 2 h to ensure the detection of any significant degree of deactivation. The tubing, which conducted the products to the gas chromatograph (type: Perkin Elmer 8500), was heated to approximately 120°C to avoid condensation. The products were separated by two columns: "Reoplex" on "Chromosorb P" (length: 2 m) as precolumn and "Poropak QS" (length: 1.5 m) as main column, followed by a methanator. Nitrogen was used as carrier gas. The column temperature was held at 40°C for 5 min and then increased at a heating rate of 10°C/min to 170°C, where it was held for 80 min. The products were detected by a flame ionisation detector (FID). In addition, nonvolatile products were condensed in a trap cooled with solid CO_2 to make a separate analysis using a gas chromatograph with a capillary column to separate the products and a mass spectrometer for analysis.

To check for diffusion limitation measurements were performed using 0.6 and 1.8 g of catalyst, holding the contact time constant. No difference in ethane conversion or selectivities to products was detected. The catalytic properties for the conversion of ethene were determined using a total pressure of 2 MPa in the range 180–260°C with a gas mixture comprising 37.5% ethene/balance air. The carbon balance was always checked and found to be better than 97%.

3. RESULTS

3.1. Reducibility of the Catalysts

Figure 1 gives the reduction profiles for the model catalysts. It can be seen, that the multiphase catalyst is much more reducible in the analysed temperature range than the other model catalysts. Of the crystalline phases found in the multiphase catalyst ($Mo_6V_9O_{40}$, $Mo_3Nb_2O_{11}$, and MoO_3; see (5)), $Mo_6V_9O_{40}$ is the most easily reduced, while MoO_3 and $Mo_3Nb_2O_{11}$ showed about the same lower reducibility. V_2O_5 showed the largest amount of reduction of all crystalline phases analysed. $NbVO_4$ seemed to be stable under these conditions.

TABLE 1

Temperatures of First Reduction ($T_{red.}$) of the Multiphase Catalyst and the Crystalline Phases

Phase	Multi-phase	$Mo_6V_9O_{40}$	$Mo_3Nb_2O_{11}$	$NbVO_4$	MoO_3	V_2O_5	Nb_2O_5
$T_{red.}$ [°C]	425	475	575	>600	575	500	600

The temperatures at which reduction was first observed are given in Table 1. It can be seen that the reduction of the multiphase catalyst starts at lower temperatures than the reduction of the crystalline phases. In the case of MoO_3 a slight reduction was detected at 425°C, but the amount was very small, going down to zero again with rising temperature, so this has been neglected in Table 1.

Because of the special interest in the phase $Mo_6V_9O_{40}$, the only crystalline phase found to catalyse the oxidation of ethane to acetic acid as will be shown later, the experimental conditions were changed to get information about the reducibility of this phase at lower temperatures. For this, the concentration of hydrogen in the reducing atmosphere was increased from 6.5 to 100%, as shown in Fig. 2. The results indicate that the phase $Mo_6V_9O_{40}$, when calcined

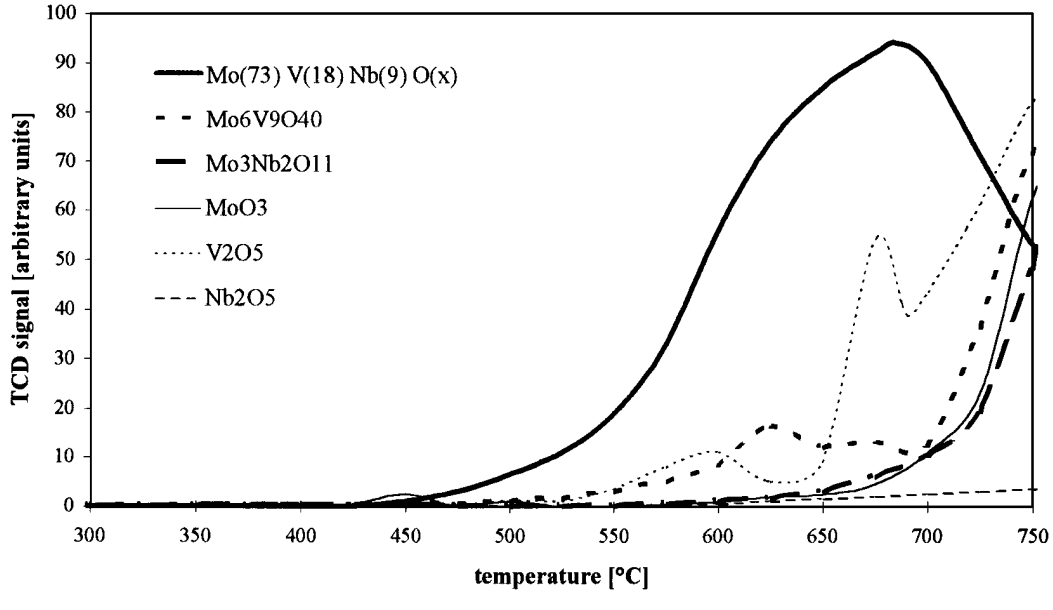

FIG. 1. Temperature-programmed reduction curves of the multiphase catalyst and the crystalline phases. Experimental conditions: heating rate, 15°C/min; atmosphere, 6.5% H_2; balance, He; $m_{sample} = 50$ mg.

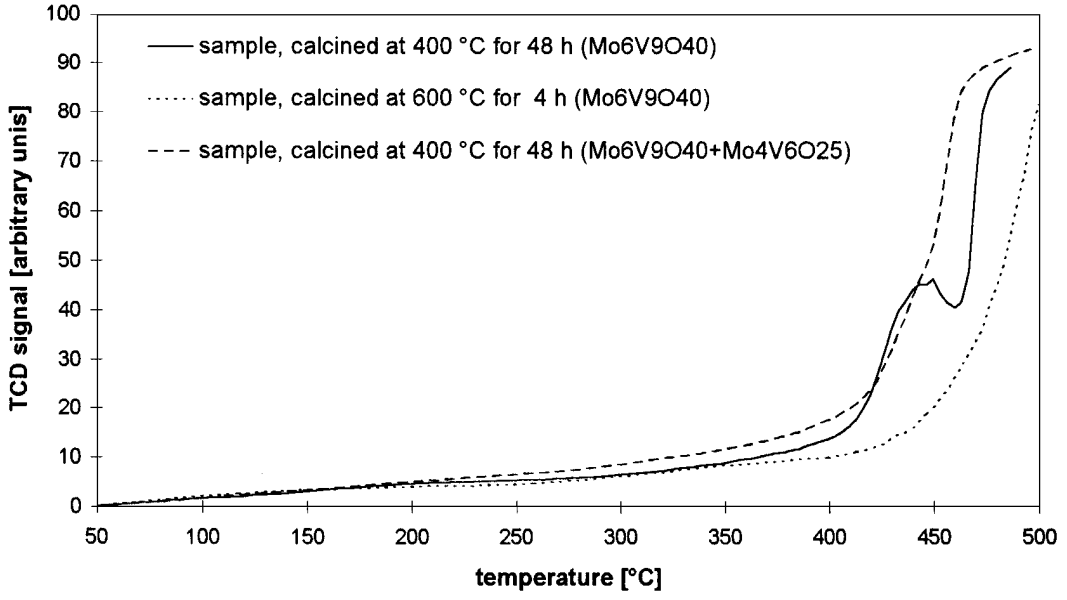

FIG. 2. Temperature-programmed reduction curves of $Mo_6V_9O_{40}$, calcined at different temperatures. One phase contains, in addition, $Mo_4V_6O_{25}$. Experimental conditions: heating rate, 15°C/min; atmosphere, 100% H_2; $m_{sample} = 200$ mg.

at 600°C, is more difficult to reduce than the sample calcined at 400°C. The latter showed a shoulder in its curve at 440°C. XRD measurements confirmed this result of different reducibility, showing the reduced samples to consist of $Mo_4V_6O_{25}$ and MoO_2 (in the case of the 600°C calcined sample) and MoO_2 (for the 400°C calcined sample).

3.2. Acidity of the Catalysts

The acidity determinations by ammonia TPD measurements for the multiphase catalyst and the crystalline phases are given in Fig. 3. The corresponding peak areas are given in Table 2 in a normalised form, setting the peak area

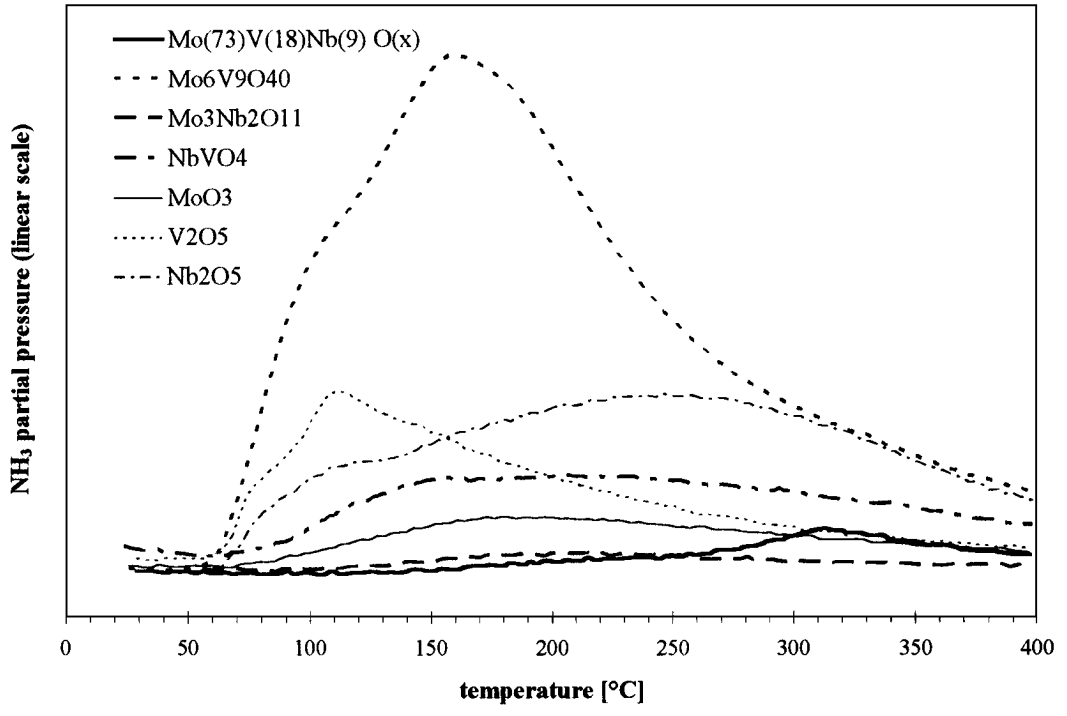

FIG. 3. NH_3 temperature-programmed desorption curves of the multiphase catalyst and the crystalline phases.

TABLE 2

Peak Areas and Characteristic Temperatures of Ammonia-Desorption Curves of the Multiphase Catalyst and the Crystalline Phases

Phase	Mo(73)V(18)Nb(9)O(x)	$Mo_6V_9O_{40}$	$Mo_3Nb_2O_{11}$	$NbVO_4$	MoO_3	V_2O_5	Nb_2O_5
$P_{absolute}$	1.0	14.1	0.7	3.3	1.8	3.5	7.3
$P_{surface}$	1.0	7.3	3.6	4.9	4.3	8.5	27.1
T_{start} [°C]	160	60		60	60	60	60
T_{max} [°C]	310	155		155–215	185	110	245

Note. $P_{absolute}$ = absolute normalised peak area; $P_{surface}$ = surface area corrected normalised peak area. T_{start} = temperature, at which first desorption was observed; T_{max} = temperature of maximum desorption rate.

corresponding to the multiphase catalyst equal to 1. All samples were analysed by XRD before and after the ammonia experiments; no change in crystalline structure was observed.

The multiphase catalyst showed only a small NH_3-desorption peak. Most of the single phase materials released a larger amount of NH_3. An exception was $Mo_3Nb_2O_{11}$, for which nearly no ammonia desorption was observed, and which will for that reason not be discussed further. These results have to be corrected for the different surface areas of the samples (Table 2). From the corrected values it follows that the multiphase catalyst has the lowest acid site concentration of all samples, while Nb_2O_5 has the highest concentration, followed by V_2O_5 and $Mo_6V_9O_{40}$.

If we examine the temperature of the start of NH_3 desorption (see Table 2) we see that the multiphase catalyst is distinctive with a rather high temperature of about 160°C. This fact, together with the observation of a desorption rate maximum at 310°C, indicates a high strength of all acid sites present. While the NH_3 desorption from all the pure crystalline phases started at the same low temperature of 60°C, the desorption temperature ranges were different. From this we conclude that acid sites of low strength exist in each of these cases, but the overall acid strength distribution varies. While V_2O_5 showed a desorption maximum at 110°C with a clearly declining desorption curve at higher temperatures, $NbVO_4$, and even more so Nb_2O_5, showed very broad desorption maxima at higher temperatures, indicating a wide distribution of acid site strengths.

3.3. Catalytic Activity in Ethane Oxidation

The influence of the different reaction parameters on the catalytic activity of the multiphase catalyst and the various crystalline phases was determined.

For the multiphase catalyst, ethane conversion strongly increases up to a temperature of 300°C, as shown in Fig. 4. Further increase of the temperature does not lead to a higher total conversion.

The temperature dependence of the yields of various products obtained for the multiphase catalyst is shown in Fig. 5. It can be seen that the yield of acetic acid is always quite low but goes through a maximum at about 240°C, while the yield of ethene reaches a larger maximum at about 270°C. At 400°C ethene and acetic acid are no longer observed in significant amounts and total oxidation to CO and CO_2 is observed. Trace amounts of acetaldehyde and ethanol, together with minor quantities of unknown products have been detected, but the selectivity to all these by-products together was always lower than 0.4%, and none of these were found at temperatures below 300°C. For this reason these products were considered to be unimportant and so they will be ignored.

The pressure dependence of the catalytic properties at a constant molar flow rate is given in Fig. 6 (full curves). The conversion was found to increase with increasing pressure, as was the selectivity to acetic acid. In particular, the increase from 0.1 to 0.5 MPa pressure is very marked. The selectivity to ethene, in contrast, decreases with increasing pressure, but, because the ethane conversion increases rapidly, the yields to the various products all increase with increasing pressure. Therefore, a high pressure is favourable for acetic acid formation. If, however, the pressure is decreased again under constant contact time (i.e., constant volumetric flow rate; see dotted curves in Fig. 6), the conversion is further increased without any remarkable change of the selectivities. This shows the pressure dependence of the reaction under constant molar flow rate mainly to be due to a changed contact time.

The influence of the gas feed composition at a pressure of 2 MPa is given in Fig. 7. With the exception of the data point to the extreme left the measurements reflect reaction under reducing conditions. With increasing ethane concentration the conversion strongly decreases. This correlates well with results in the literature (2). However, at this higher pressure the influence on the selectivities was very small. While the selectivity to acetic acid increased slightly with increasing ethane content in the feed, the selectivity to ethene remained stable. The yields to ethene and acetic acid both decrease with increasing ethane concentration.

The dependence of the ethane conversion and the selectivities on the contact time is given in Fig. 8 and this shows a continuous increase of the ethane conversion with increasing contact time. The behaviour of the selectivities is varied:

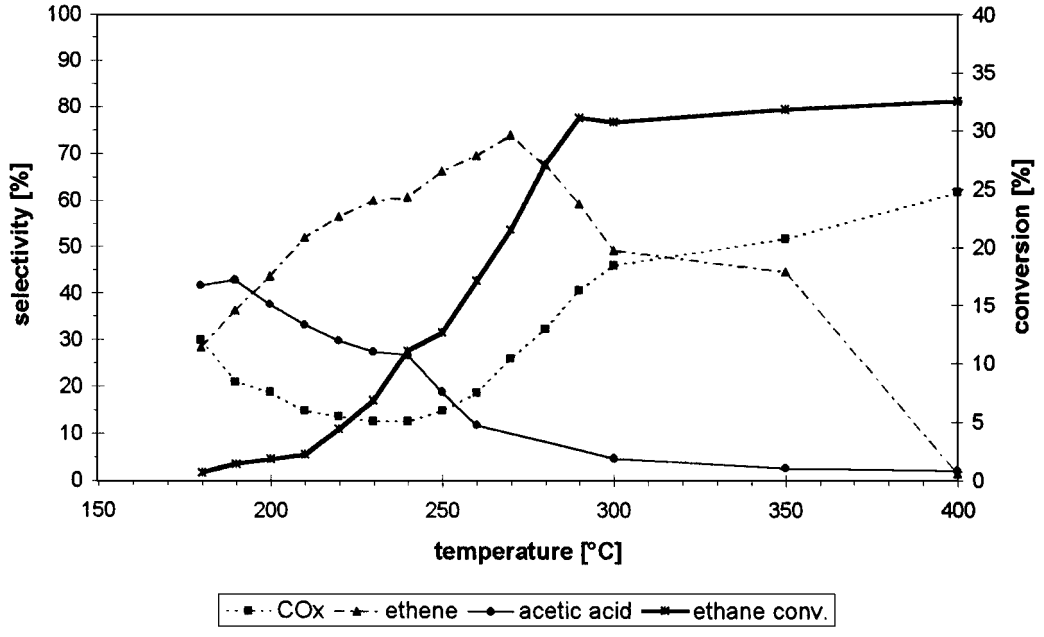

FIG. 4. Multiphase catalyst: selectivities and conversions as a function of temperature at a pressure p of 2 MPa after t = 12 h at each temperature. Gas feed: 25% ethane in air; contact time $\tau = 79$ s.

while the selectivity to ethene decreases, the selectivities to total combustion products is enhanced by increasing the contact time. The selectivity to acetic acid remains unaffected by contact time changes within the limits of accuracy of the measurements. A linear extrapolation to zero contact time under the conditions of Fig. 8 was used to determine the approximate concentrations of the primary products at 240°C and a pressure of 2 MPa. This gave: 73% ethene, 23% acetic acid, and 4% total combustion products.

In Fig. 9 the catalytic properties for the ethane conversion of the multiphase catalyst and the various crystalline phases are presented for comparison for a temperature of 240°C, the optimum temperature for acetic acid formation over the multiphase catalyst, and a pressure of 2 MPa. The conversions have been corrected for variations in the surface areas of the catalysts. From this diagram it is clear that the multiphase catalyst is more active than the crystalline phases, with the exception of V_2O_5. For all the crystalline

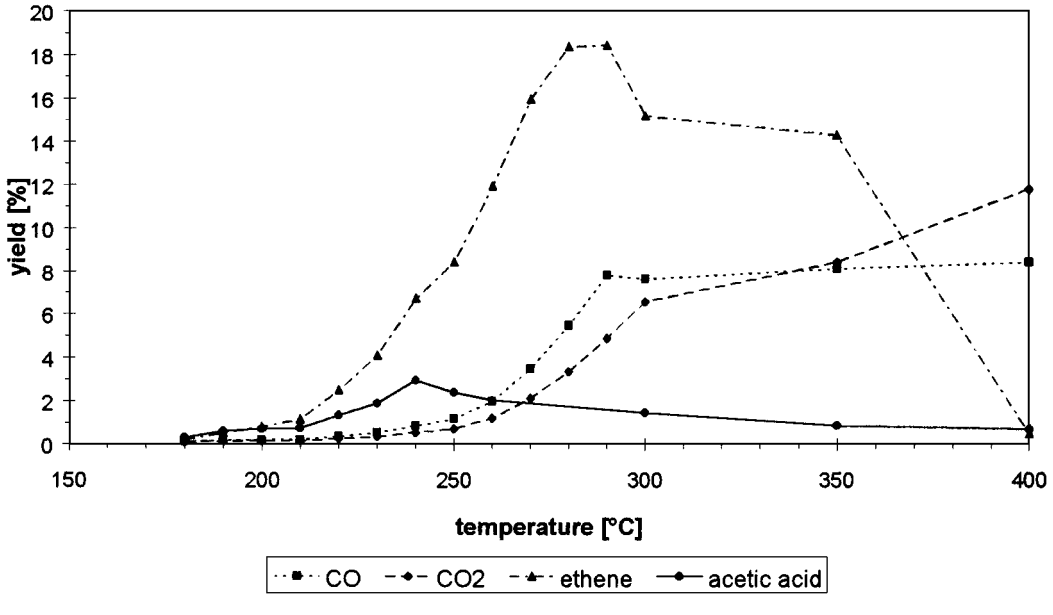

FIG. 5. Multiphase catalyst: yields as a function of temperature.

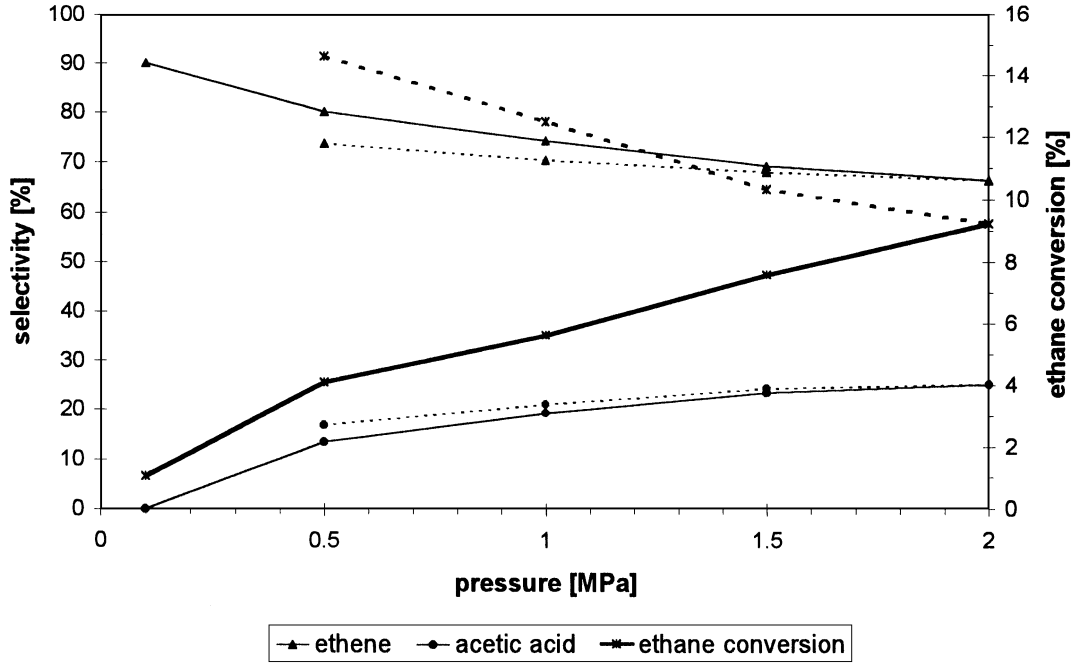

FIG. 6. Multiphase catalyst: selectivities and ethane conversion as a function of pressure at T = 240°C (full lines, molar flow rate constant; dotted lines, volumetric flow rate constant; $\tau = 79$ s). Gas feed (see Fig. 4).

phases total combustion was by far the most dominant reaction, but some ethene was also always found. Acetic acid was only produced by the multiphase catalyst and the phase $Mo_6V_9O_{40}$, but the selectivity and yield for the latter were already much smaller than those obtained with the multiphase catalyst. The experiments with $Mo_3Nb_2O_{11}$ and MoO_3 were the only ones where other oxidation products in measurable amounts were found. In the case of MoO_3, this was acetaldehyde, and in the case of $Mo_3Nb_2O_{11}$, acetaldehyde, and acetone. MoO_3 was found to be primarily a total combustion catalyst (about 97% of the ethane underwent total combustion), leading mainly to CO_2, and although the

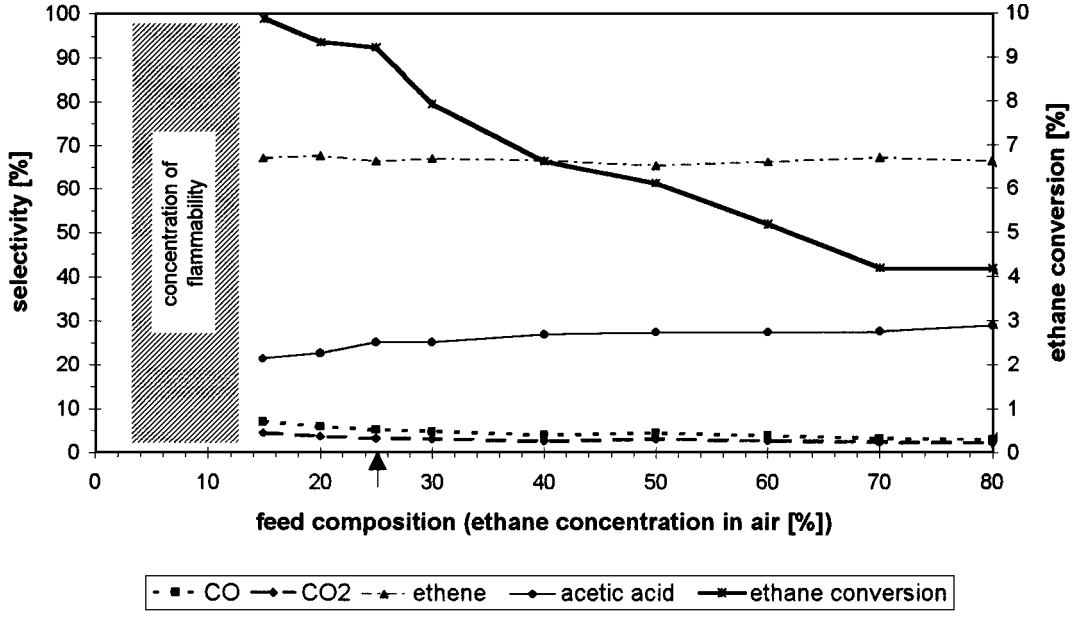

FIG. 7. Multiphase catalyst: selectivities and ethane conversion as a function of feed composition (T = 240°C, p = 2 MPa, $\tau = 79$ s). The shaded area represents the region of flammability at atmospheric pressure.

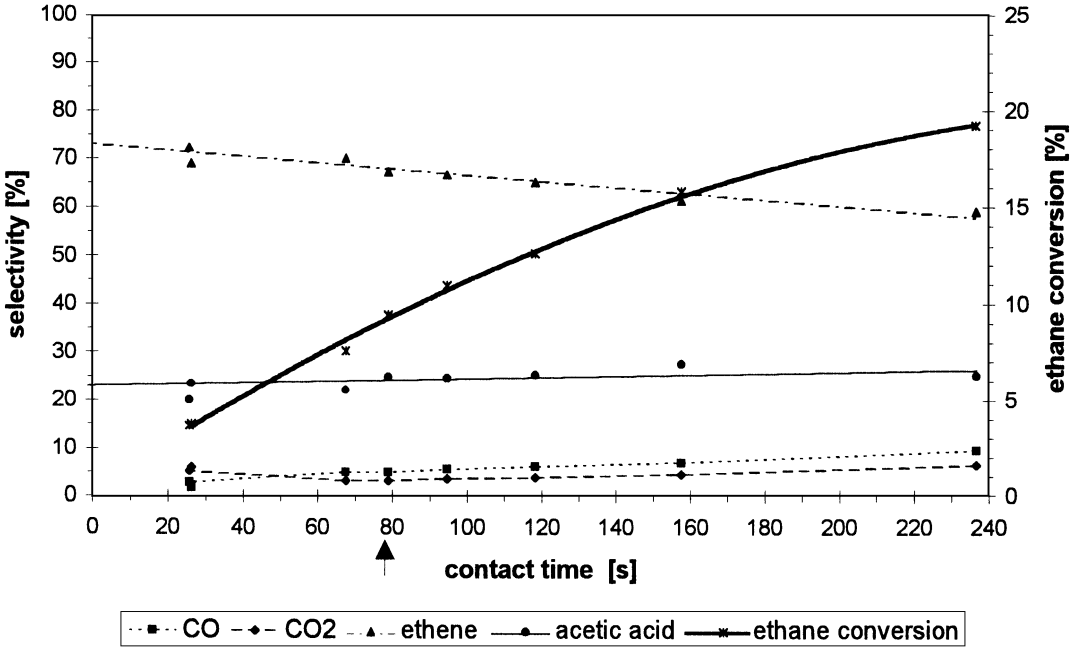

FIG. 8. Multiphase catalyst: selectivities and ethane conversion as a function of contact time (T = 240°C, p = 2 MPa). Gas feed (see Fig. 4).

phase $Mo_6V_9O_{40}$ catalysed the formation of ethene as well as acetic acid the main product was CO_x over the whole temperature range.

3.4. Catalytic Activity in Ethene Oxidation

The aim of these experiments was to obtain information about the possible mechanism for acetic acid formation and to compare the catalytic properties of the different model catalysts for ethane and for ethene activation. Catalytic tests were performed with the multiphase catalyst and the crystalline phases found in it, i.e. $Mo_6V_9O_{40}$, MoO_3, and $Mo_3Nb_2O_{11}$.

The results of the catalytic test with the multiphase catalyst for the conversion of ethene in air are given in Fig. 10. Up to 210°C most of the converted ethene underwent total combustion, but at higher temperatures acetic acid

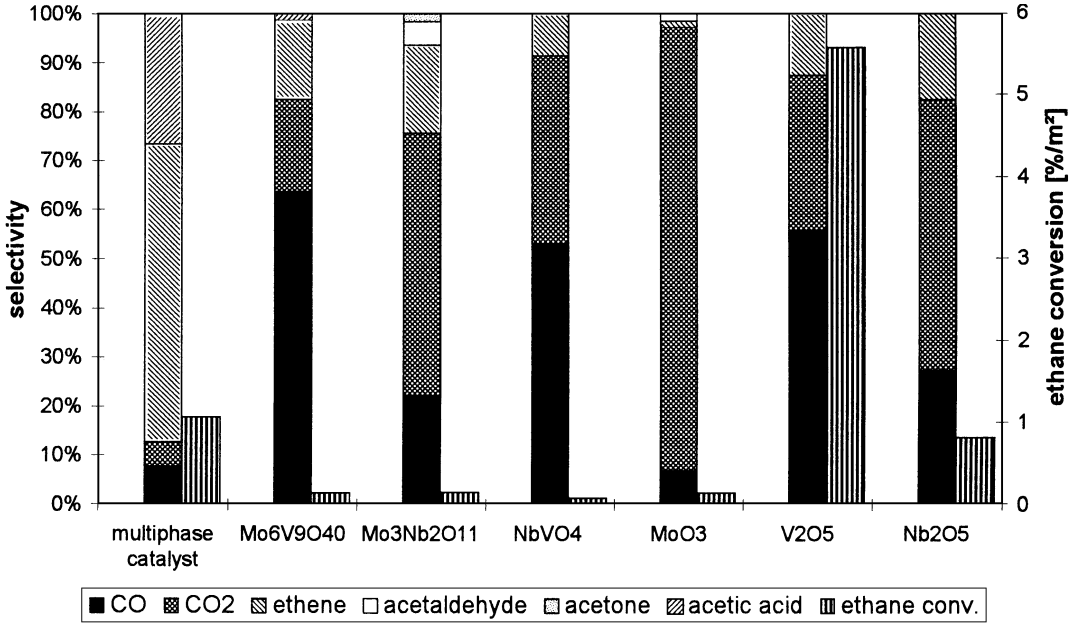

FIG. 9. Comparison of the catalytic properties of the multiphase catalyst and the crystalline phases at 240°C and a pressure of 2 MPa. Gas feed: 25% ethane in air, $\tau = 79$ s. The conversion is calculated per unit surface area.

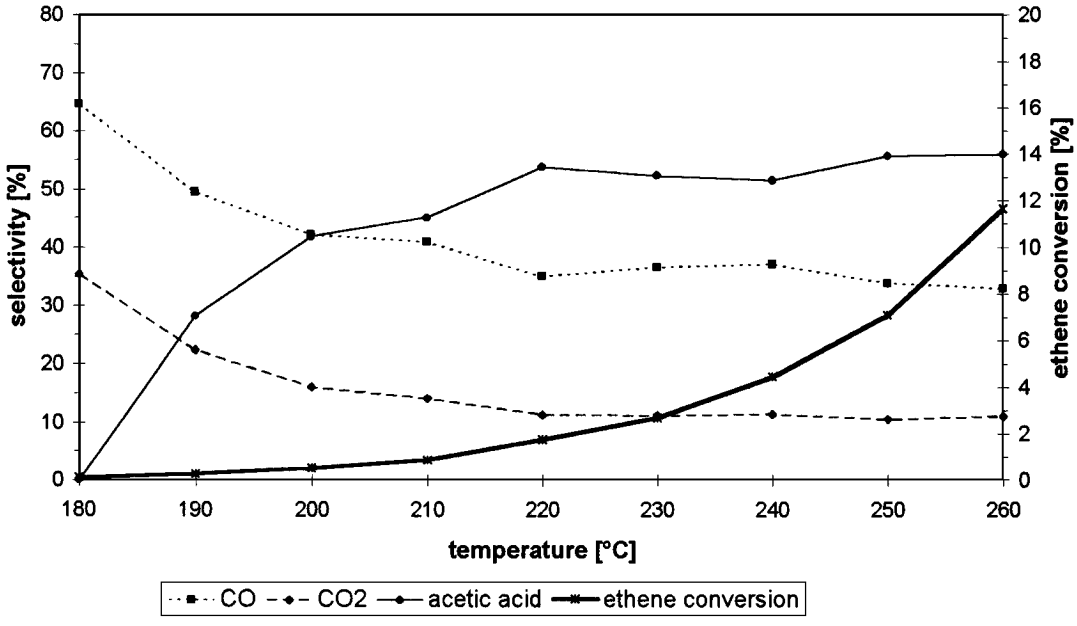

FIG. 10. Multiphase catalyst: selectivities and ethene conversion as a function of temperature at p = 2 MPa. Gas feed: 37.5% ethene in air, $\tau = 79$ s.

formation became dominant. Above 220°C the selectivities did not change significantly.

In comparison with the multiphase catalyst (Fig. 10) the crystalline phase $Mo_6V_9O_{40}$ was much more active (see Fig. 11). Up to a temperature of 240°C the ethene conversion was found to be nearly five times higher than was observed with the multiphase catalyst. Although the selectivity to acetic acid decreased with temperature, up to 240°C the yield to acetic acid was about two to three times higher than that obtained with the multiphase catalyst.

MoO_3 converted ethene to acetone, acetaldehyde, and an unidentified product. Acetic acid was only formed at temperatures above 260°C. $Mo_3Nb_2O_{11}$ did not catalyse the formation of acetic acid. The only products found, besides CO_x, were acetaldehyde, acetone, and one unknown product. While acetaldehyde appeared already at a reaction

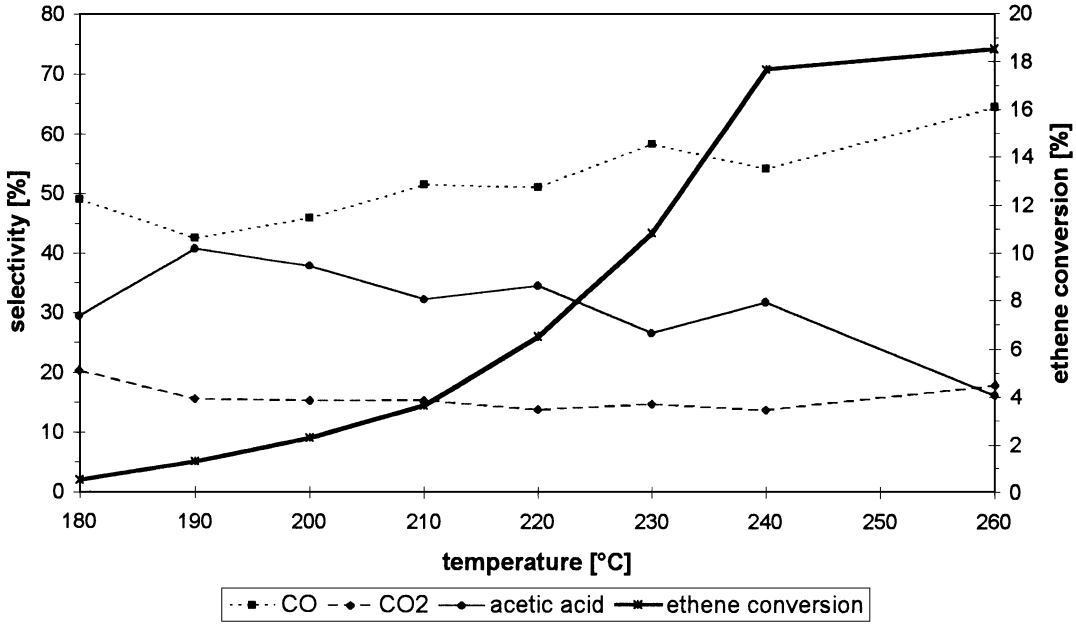

FIG. 11. $Mo_6V_9O_{40}$: selectivities and ethene conversion as a function of temperature at p = 2 MPa. Gas feed: 37.5% ethene in air, $\tau = 79$ s.

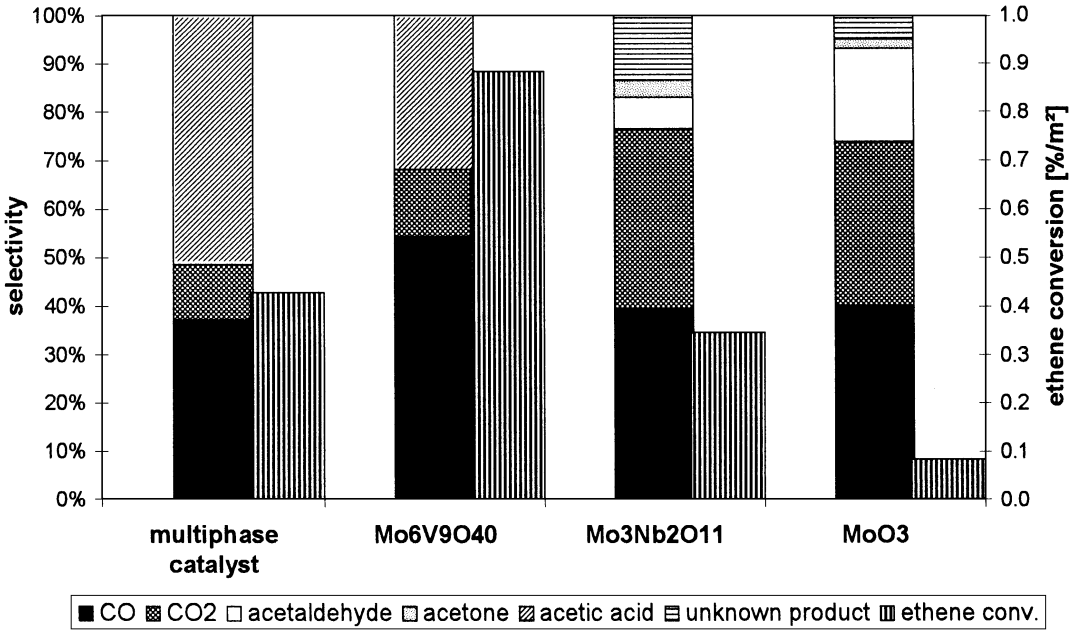

FIG. 12. Comparison of the catalytic properties of the multiphase catalyst and its crystalline phases for the conversion of ethene at 240°C and a pressure of 2 MPa. Gas feed: 37.5% ethene in air, $\tau = 79$ s. The conversion is calculated per unit surface area.

temperature of 200°C, reaching its maximum selectivity at 230°C, the formation of acetone began at a slightly higher temperature, increasing continuously up to 260°C. Mass spectrometric analysis of the liquid products condensed at −78°C, showed the product to contain traces of propionic acid, formaldehyde, maleic anhydride, and products of heavier molecular weight, from which one is possibly the unknown product already detected by gas chromatography.

In Fig. 12 the catalytic properties of the multiphase catalyst and its crystalline phases for the catalytic conversion of ethene in air are compared. We see that the results are very different from those obtained with ethane in the feed (Fig. 9). The multiphase catalyst and the phase $Mo_6V_9O_{40}$ are the only samples which make significant amounts of acetic acid. $Mo_3Nb_2O_{11}$ and MoO_3 form acetaldehyde, acetone, and one unidentified product; none of these products are found in a significant amount with the multiphase catalyst and $Mo_6V_9O_{40}$.

A comparison of the results (Figs. 9 and 12) with ethane or ethene in the feed shows that the activities are very different. While in the case of ethane the multiphase catalyst was far more active than the phase $Mo_6V_9O_{40}$ the latter is the most active with ethene. It is interesting to note that the selectivity to acetic acid is increased in the case of both catalysts although the increase obtained with $Mo_6V_9O_{40}$ is particularly large.

4. DISCUSSION

We know from X-ray diffraction and analytical electron microscopy experiments that the multiphase catalyst consists of at least three different crystalline phases ($Mo_6V_9O_{40}$, $Mo_3Nb_2O_{11}$, and MoO_3) and possibly other phases of poor crystallinity or amorphous structure (5). Therefore, the morphology of these samples can be expected to be complex. Our characterisation results will be used as far as possible to provide explanations for the different catalytic properties of the various catalysts. To facilitate this understanding a summary of the key points from the catalytic experiments are collected together in Table 3.

The first point to consider is the activation of the hydrocarbon molecules and for this purpose acidity measurements have been found to be useful. There are two possibilities for the C–H bond splitting during adsorption: *homolytic* rupture, leading to neutral adsorbates, and *heterolytic* splitting, forming ionic adsorbates. While homolytic splitting is normal on metal surfaces, for oxidic catalysts the acid–base properties of the catalyst surface and of the adsorbate become important.

A comparison of the catalytic conversion of ethane and ethene over the multiphase catalyst and the phase $Mo_6V_9O_{40}$ showed that while over the multiphase catalyst the total conversion of ethane was higher than that of ethene, the phase $Mo_6V_9O_{40}$ gave greater activation of ethene than of ethane which may reflect the higher acidity of this material.

In addition to the activity differences observed for ethane and ethene it is also interesting to note that the acetic acid yield is higher in both cases with ethene as reactant. This might be interpreted as evidence that the formation of acetic acid involves ethene as an intermediate.

TABLE 3

Summary of the Most Important Results Obtained by Catalytic Testing of the Model Catalysts

Phases identified	Surface area (m^2/g)	Conversion of		Products found				
		Ethane (%/m^2)	Ethene (%/m^2)	Ethene	Acetic acid	Acetaldehyde	Acetone	Unknown product
$Mo_6V_9O_{40}$, $Mo_3Nb_2O_{11}$, MoO_3 (multiphase catalyst)	10	1.06	0.43	X	X, O			
$Mo_6V_9O_{40}$	20	0.14	0.88	X	X, O			
$Mo_3Nb_2O_{11}$	2	0.14	0.35	X		X, O	X, O	O
$NbVO_4$	7	0.08	—	X				
MoO_3	4	0.13	0.08	X		X, O	O	O
V_2O_5	4	5.57	—	X				
Nb_2O_5	3	0.81	—	X				

Note. X = with a feedstock of ethane and air; O = with a feedstock of ethene and air; — = no measurements taken.

However, the effect of contact time on the product distribution (see Fig. 8) suggests that this is not correct.

A change in the crystallinity of the multiphase catalyst was especially noticeable when increasing the calcination temperature from 400 to 500°C. Parallel with the change in crystallinity of the whole sample, a growth of the crystals was observed. Molybdenum oxide, in particular, separated out when the temperature was increased from 400 to 500°C. The same might be true for the phase $Mo_3Nb_2O_{11}$. Therefore, a possible explanation for the strong decrease in activity of the catalyst when calcined at 500°C, instead of 400°C, might be the destruction of an active amorphous phase by loss of molybdenum and niobium.

The *temperature programmed reduction (TPR)* measurements have shown that the multiphase catalyst and the phase $Mo_6V_9O_{40}$ started to be reduced at lower temperatures $T_{red.}$ than the other samples (compare Table 1). $T_{red.}$ is a measure of the ease of oxygen removal from the catalyst. The multiphase catalyst and the phase $Mo_6V_9O_{40}$ are the only two samples catalysing the formation of acetic acid. It seems, therefore, that in the formation of acetic acid the hydrogen abstraction and oxygen insertion reactions can be correlated with sites which can provide lattice oxide ions under reaction conditions.

An example of the importance of lattice oxygen for the oxidation of ethane to acetic acid can be found by comparing Mo_5O_{14} with a catalyst comprising MoO_2, which has the rutile structure. In this structure the oxygens form a deformed hexagonal dense packing, in which every second octahedral hole is occupied by a molybdenum ion (7). This structure neither contains molybdenum in the intermediate oxidation state Mo^V to activate ethane, nor does it provide weakly bonded oxygens. The phase Mo_5O_{14} is a metastable phase which decomposes under prolonged heat treatment into $Mo_{17}O_{47}$ and MoO_3 (8, 9), but it has been found to be stable when a small part of the molybdenum is substituted with vanadium (9), or niobium (10).[1] This phase contains $Mo^{V\,2}$ centres and oxide ions which are more easily removable than those found in MoO_2. It might be concluded, therefore, that the phase Mo_5O_{14} is more suitable for the selective ethane oxidation than MoO_2 due to its ability to both activate the ethane molecule and to provide lattice oxygen (compare (3)).

The phase $Mo_6V_9O_{40}$ was found to be the only pure oxidic phase catalysing the formation of acetic acid. The reason might be that not all cations are oxidised to their highest oxidation state. This would correlate well with the results of Thornsteinson *et al.* (1) who ascribe the activity of the multiphase catalyst to the presence of Mo^V, which was found to be present in the freshly prepared catalyst, but to disproportionate under the influence of ethane to Mo^{IV} and Mo^{VI}. Finally, Mo^{VI} was seen to form the active sites, but it would have to be in an environment deficient in oxygen, created by Mo^V disproportionation. In this respect, note the stabilisation of Mo^V by Nb as mentioned above.

For heterogeneously catalysed oxidation processes the Mars and van Krevelen mechanism (11), dividing the process into an oxidation step of the adsorbed molecule with local reduction of the catalyst, and the separate reoxidation of the catalyst, is widely accepted. Therefore, the following discussion will focus on this type of surface reaction.

Figure 13 gives the mechanism for the selective oxidation of ethane, summarised from various literature references. The ethane molecule is adsorbed on the catalyst surface in the form of an ethoxide species, as proposed for the case of V^V by Oyama (12) or for the case of Mo^{VI} by Thornsteinson *et al.* (1). This ethoxide species can then become an ethene

[1] For vanadium a homogeneity range was found given by: $(Mo_{1-x}V_x)_5O_{14}$ with $x = 0.02 \leq x \leq 0.11$ (9). For niobium the compositions with $(Mo_{1-x}Nb_x)_5O_{14}$ with $x = 0.09$ and 0.40 were found to be stable (10).

[2] Mo_5O_{14} corresponds to $Mo_3^{VI}Mo_2^{V}O_{14}$.

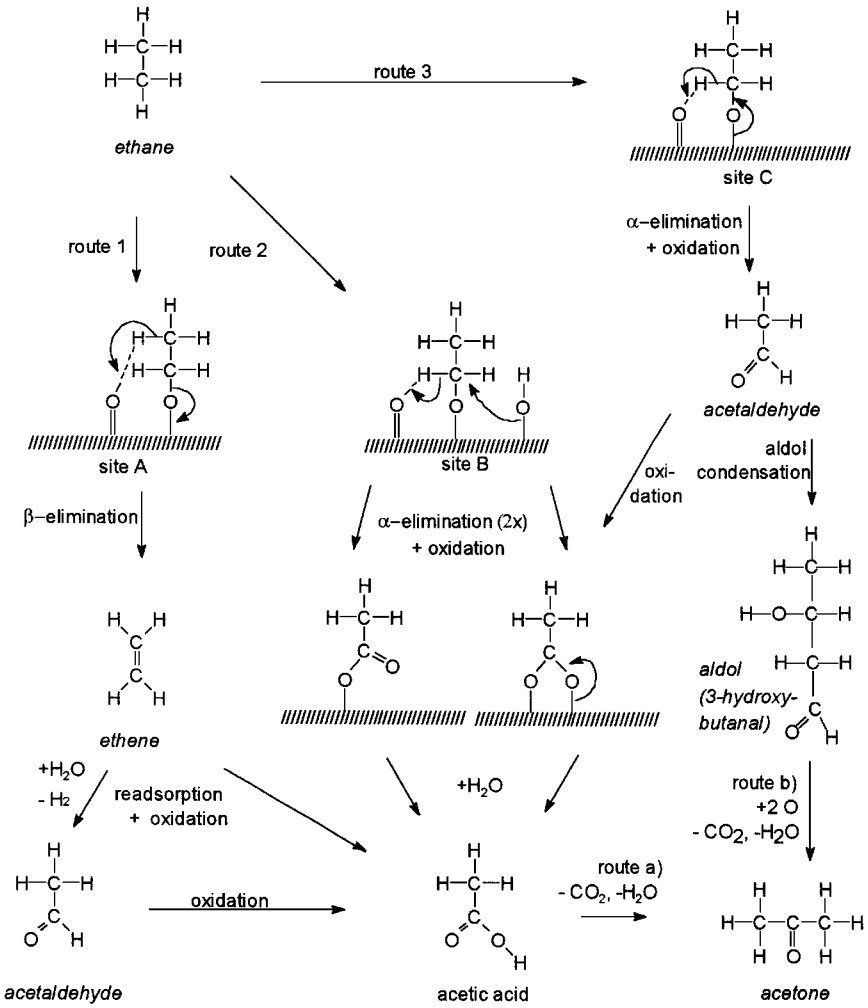

FIG. 13. Possible mechanism for the selective oxidation of ethane, as found in literature (references: see text).

molecule by β-elimination (route 1) (1, 12). The hydrogen to be abstracted can be bound to the catalyst surface; geometrical considerations for the exact mechanism can be found in Refs. (1) and (13). Further readsorption of the ethene molecule to a catalyst cation could lead to oxidation to acetaldehyde or acetic acid (14), but this is not found to be an important mechanism for the formation of acetic acid (15). Acetaldehyde, formed from ethene under the presence of water involving ethanol as intermediate, could also be oxidised to acetic acid (16). If the ethoxide species undergoes α-elimination, acetaldehyde and acetic acid can be formed directly (route 2 (3) and route 3 (12)). The catalyst would have to be reoxidised in a different step (17). The α- and β-eliminations are probably catalysed on different sites (3), and also the α-elimination processes to acetic acid and acetaldehyde might involve different sites.

The formation of acetic acid requires, in addition to two α-elimination steps, a coordination of a hydroxyl group to the α-carbon, followed by adsorption on two surface oxygens, partial desorption through the formation of the carbonyl group, and desorption with the participation of a free water molecule according to the scheme (15):

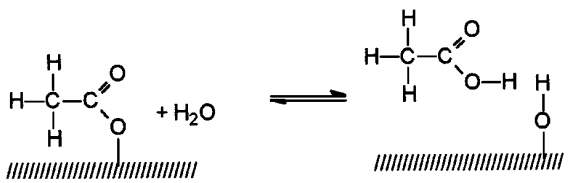

In Ref. (15) it is noted that the desorption of acetic acid might be the rate-determining step as water in the gas feed improves the selectivity to acetic acid over a vanadium oxide catalyst, which is seen to be due to a shift of the desorption–adsorption equilibrium to the desorption side. Desorbed acetaldehyde, as an intermediate for a subsequent second oxidation step to acetic acid is possible, but it is more likely to undergo total combustion when activated

by surface oxygen. Condensation with a second acetaldehyde molecule to aldol is proposed in the literature (18, 19). A final oxidation step could then lead to acetone, releasing the excess carbon and hydrogen in the form of CO_2 and water (18, 19).

The catalytic test of the multiphase catalyst as a function of contact time (Fig. 8) suggests that ethene is not an intermediate in the formation of acetic acid as changes in ethene selectivity are not reflected in changes in acetic acid selectivity. As can be seen from Fig. 9, all catalysts led to the formation of ethene. Acetic acid or acetaldehyde, in contrast, were only found in the case of the multiphase catalyst and its crystalline phases ($Mo_6V_9O_{40}$, MoO_3, and $Mo_3Nb_2O_{11}$). The α-elimination, leading to acetic acid and acetaldehyde, was a low temperature process, while the β-elimination, resulting in the formation of ethene, was shown to be favoured by higher temperatures (Fig. 4). The activation energy can, therefore, not be the reason for the hindrance of the α-elimination on the surfaces of $NbVO_4$, V_2O_5, and Nb_2O_5. The need for specific types of sites provides a possible explanation. This supports the assumption that α- and β-elimination are catalysed by two different sites.

$Mo_3Nb_2O_{11}$ and MoO_3 were the only samples to catalyse the formation of acetaldehyde (Fig. 9). This might mean that these catalysts support the oxidation to acetaldehyde, but not the two-step oxidation to acetic acid. There are two possible explanations why no acetaldehyde is found among the products formed over the multiphase catalyst, although it contains the phases $Mo_3Nb_2O_{11}$ and MoO_3: the acetaldehyde may react further on other sites to total combustion products, or the fraction of the total surface area of the multiphase catalyst which is due to MoO_3 and $Mo_3Nb_2O_{11}$ may just be too small to make a significant contribution to the total activity of the catalyst.

5. CONCLUSIONS

This work has shown that the catalytic activity of the catalyst Mo(73)V(18)Nb(9)O(x) cannot be ascribed only to the identified crystalline phases. Although these showed very different catalytic activities, amorphous phases are present and cannot be neglected. The contribution of the different catalytic phases to the total activity of the catalyst is determined by the catalytic properties of the material and by the surface area of each phase present. Electron microscopy shows that the largest fraction of the surface area of the catalyst belongs to an amorphous or very poorly crystallised part of the catalyst. Most of the grains of this part were identified to be of the composition $Mo(84 \pm 3)V(13 \pm 3)Nb(2 \pm 0.5)O(x)$. This phase can be assumed to contribute the largest part to the favourable selective catalytic properties of the catalyst, although synergistic effects between different phases cannot be excluded. The role of niobium can be seen in the stabilisation of this amorphous phase. For this to occur the Nb has to be introduced during the preparation of the sample. Treatment of the catalytically active phase $Mo_6V_9O_{40}$ with a niobium-containing solution did not improve its catalytic properties.

To preserve this active, amorphous phase, the calcination temperature has to be kept low (e.g., 400°C) to prevent separation into the different crystalline phases, as was observed by electron microscopy. This again makes an adequate preparation of the precursor necessary to allow the formation of the active phase at this low temperature.

The two reactions of interest, the dehydrogenation of ethane to ethene and the oxidation to acetic acid, were catalysed by the various crystalline phases ($Mo_6V_9O_{40}$, $Mo_3Nb_2O_{11}$, $NbVO_4$, MoO_3, V_2O_5, Nb_2O_5) to different extents. While all crystalline phases catalyse the dehydrogenation of ethane to ethene, only $Mo_6V_9O_{40}$ allowed the oxidation to acetic acid.

Using the multiphase catalyst, the influence of the *reaction parameters* was determined. Over a wide reaction parameter range both reactions of interest can be observed. However, optimum conditions are different. Under our conditions ($p = 2$ MPa, contact time $= 79$ s) the reaction *temperature* for an optimum product yield has been found to be: 280°C for the formation of ethene and 240°C for the formation of acetic acid.

Variation of the *pressure* demonstrated that for a maximum product yield a high pressure is favourable in the case of both products, but the selectivities are influenced differently. With increasing pressure the selectivity to ethene decreased, while the selectivity to acetic acid increased. The positive influence of an elevated pressure can mainly be assigned to an increase of the contact time. The influence of the *contact time* was analysed, holding temperature and pressure constant ($T = 240$°C, $P = 2$ MPa). While an increasing contact time caused part of the ethene formed to undergo total combustion, the selectivity to acetic acid remained unaffected. This means that acetic acid, once it is formed, is stable.

Correlations between the material properties and the catalytic activity have been noted, and there were particular indications for the importance of:

- acidity for the activation of the ethane molecule;
- low temperature reducibility for the oxidation to acetic acid;
- microscopic morphology for the contribution of the various parts of the catalyst to the total catalytic activity and the stability of the catalyst.

ACKNOWLEDGMENTS

We are pleased to acknowledge financial support from the EU through the Human Capital and Mobility Programme "Catalytic Functionalisation of Lower Hydrocarbons," Contract CHRX CT920065.

REFERENCES

1. Thornsteinson, E. M., Wilson, T. P., Young, F. G., and Kasai, P. H., *J. Catal.* **52**, 116 (1978).
2. Burch, R., and Swarnakar, R., *Appl. Catal.* **70**, 129 (1991).
3. Merzouki, M., Taouk, B., Monceaux, L., Bordes, E., and Courtine, P., *in* "New Developments in Selective Oxidation by Heterogeneous Catalysis," p. 165. Elsevier Science, Amsterdam, 1992. [Studies in Surface Science and Catalysis, Vol. 72]
4. Despons, O., Keiski, R. L., and Somorjai, G. A., *Catal. Lett.* **19**, 17 (1993).
5. Ruth, K., Kieffer, R., and Burch, R., submitted.
6. Tanabe, K., *in* "Solid Acids and Bases," Chap. 5. Kodansha/Academic Press, Tokyo/New York, 1970.
7. Burzlaff, H., and Zimmermann, H., "Kristallsymmetrie—Kristallstruktur," Verlag Merkel, Erlangen, 1986.
8. Kihlborg, L., *Acta Chem. Scand.* **13**, 954 (1959).
9. Ekström, T., and Nygren, M., *Acta Chem. Scand.* **26**, 1827 (1972).
10. Ekström, T., and Nygren, M., *Acta Chem. Scand.* **26**, 1836 (1972).
11. Mars, P., and van Krevelen, D. W., *Chem. Eng. Sci.* **3**, 41 (1954).
12. Oyama, S. T., *J. Catal.* **128**, 210 (1991).
13. Cotton, F. A., LaCour, T., and Stanislowski, A. G., *J. Amer Chem. Soc.* **96**, 754 (1974).
14. Merzouki, M., Taouk, B., Tessier, L., Bordes, E., and Courtine, P., *in* "Proceedings, 10th International Congress on Catalysis, July 19–24, 1992, Budapest, Hungary" (L. Guczi *et al.*, Eds.), p. 753. Elsevier Science, Amsterdam, 1993.
15. Tessier, L., Bordes, E., and Gubelmann-Bonneau, M., *Catal. Today* **24**, 335 (1995).
16. Baerns, M., personnel communication.
17. Nakajima, T., Nameta, H., Mishima, S., Matsuzaki, I., and Tanabe, K., *J. Mater. Chem.* **4**(6), 853 (1994).
18. Bussi, J., Parodi, S., Irigaray, B., and Kieffer, R., *in* "Actas XV° simposium Iberoamericano de Catalisis, Sept. 15–20, 1996, Cordoba, Argentina."
19. Claridge, J. B., Green, M. L. H., Tsang, S. C., and York, A. P. E., *J. Chem. Soc. Faraday Trans.* **89**, 1089 (1993).